Network Planning With Actual Margins

Polyzois Soumplis, Konstantinos Christodoulopoulos, Marco Quagliotti, Annachiara Pagano, and Emmanouel Varvarigos

***Abstract*—To ensure uninterrupted communication in optical transport networks, the common practice is to overprovision lightpaths in terms of capacity and physical layer performance. Overprovisioning at the physical layer is achieved using worst case assumptions and high margins in the estimation of the Quality of Transmission (QoT) when provisioning lightpaths. End-of-Life system margins are used to anticipate performance deteriorations due to additional future interference, ageing, and maintenance operations, while the design margin is used to account for inaccuracies in the QoT estimation. Such assumptions decrease network efficiency and increase the network cost. The advent of elastic optical networks and software defined networking will enable a dynamically and adaptably operated optical network. We envision an optical network that continuously senses the physical layer and optimizes connections accordingly. This enables static (e.g., worst case) physical information to be replaced by the real-time (and accurate) information. We propose an algorithm that takes into account the actual physical layer performance to provision the lightpaths with actual (just enough) margins, optimizing the decisions regarding the placement and transmission parameters of transponders and regenerators including their launch powers. Using this algorithm in a multiperiod planning scenario, we quantify the cost benefits of provisioning with actual margins as opposed to planning with worst case margins.**

***Index Terms*—Elastic optical networks, lightpaths provisioning, multi-period network planning, physical layer impairments (PLIs), power optimization, quality of transmission (QoT), routing and spectrum allocation (RSA), system and design margins.**

I. Introduction

COHERENT transponders play a crucial role in the development of next generation optical networks [1]. Coherent reception combined with high-speed electronics and sophisticated Digital Signal Processing (DSP) techniques, offer an unprecedented increase in the capacity and spectral efficiency of the optical network. Although coherent DSP–based receivers are able to compensate several physical layer impairments (PLIs) that accumulate during propagation (mainly dispersion effects), the physical layer still poses important and yet unresolved issues for current and future transport systems.

Connections in optical networks, called lightpaths, have to be provisioned with acceptable Quality of Transmission (QoT). QoT estimation is typically performed when planning or upgrading the network by a Q-tool using some physical layer model. In addition to noise from amplifiers (Amplified spontaneous emission noise– ASE), dispersion effects and intra-channel non-linearities (Self-Channel Interference – SCI), the QoT of a lightpath is affected by the existence and the parameters of neighbouring lightpaths causing inter-channel interference [2]. This is modeled through PLIs, such as crosstalk (XT), Cross-Channel Interference (XCI), and Multi-Channel Interference (MCI) [21]. To complicate network planning even more, inter-channel interference increases with time, as new connections (thus, new inter-channel interference sources) are established. Moreover, two other major sources of QoT deterioration with time include equipment (fiber, transponders, amplifiers, filters/switches) ageing, and maintenance operations (e.g., reparation of fiber cuts) that accumulate additional and sometimes irregular deteriorations.

To account for these anticipated deteriorations of the QoT with time, lightpaths are typically provisioned for what is called End-Of-Life (EOL) performance, that is, with high *system margins,* chosen to guarantee acceptable QoT under worst-case interference and under pessimistic estimates for the ageing and maintenance effects expected after several years of network operation (e.g., 10 years) [3], [4]. Moreover, since QoT estimation is performed with the use of a physical layer model, the estimation is subject to inaccuracies: the model does not capture all physical details or the input, the physical parameters of the network, are not known with enough accuracy. To account for QoT estimation inaccuracies, another margin, referred to as the *design margin*, is used on top of the EOL system margins [3], [4].

In reality, however, the network operates most of the time far away from the EOL system margins; it most probably never operates under full load, not all the budgeted maintenance operations ever take place, and ageing plays a major role only during the latest years. Moreover, once lightpaths are established, their actual performance can be checked and the design margin can

Manuscript received April 14, 2017; revised June 19, 2017 and July 20, 2017; accepted August 7, 2017. Date of publication October 17, 2017; date of current version November 16, 2017. This work was supported in part by the Horizon 2020 ORCHESTRA project under Grant 645360. *(Corresponding author: Polyzois Soumplis.)*

P. Soumplis is with the Computer Technology Institute and Press – Diophantus, Patra 26333, Greece, and also with the Department of Computer Engineering and Informatics, University of Patras, Patras 26504, Greece (e-mail: soumplis@ceid.upatras.gr).

K. Christodoulopoulos is with the Computer Technology Institute and Press-Diophantus, Patra 263 33, Greece, and also with the School of Electrical and Computer Engineering, National Technical University of Athens, Athens 15780, Greece (e-mail: kchristo@mail.ntua.gr).

M. Quagliotti and A. Pagano are with the Telecom Italia, Turin 10148, Italy (e-mail: marco.quagliotti@telecomitalia.it; annachiara.pagano@telecomitalia.it).

E. Varvarigos is with the School of Electrical and Computer Engineering, National Technical University of Athens, Athens 15780, Greece, and also with the Electrical and Computer Systems Engineering, Monash University, Melbourne VIC 3800, Australia (e-mail: vmanos@central.ntua.gr).

Color versions of one or more of the figures in this paper are available online at http://ieeexplore.ieee.org.

Digital Object Identifier 10.1109/JLT.2017.2743461

be removed. The high system and design margins translate to reduced optical reach estimates used in planning, requiring the deployment of more regenerators and more robust transponders than are strictly necessary at the time of installation. So, reducing the margins can avoid the purchase of equipment, or postpone it until it is actually needed, resulting in both cases in reduced cost [6], [7]. The savings from postponing purchases come from the decrease of equipment prices as time passes and from the time value of money (present value discount rate). Moreover, more advanced equipment becomes available as time advances, implying that postponing the purchases results also in a gradual upgrade of the network.

The problem of provisioning with reduced margins becomes more relevant with the deployment of coherent receivers and the advent of Elastic optical networks (EONs) [5]. ORCHESTRA project [7] works on extending the coherent receivers to operate as optical performance monitors (OPM) and on developing a responsive and scalable monitoring and control plane as well as an optimization tool to use such data. OPMs can be used to obtain accurate estimates of the interference and ageing factors of the network and also reduce inaccuracies in QoT estimation [3], [4], [9] so that lightpaths use *actual* (*just enough*) margins, when new ones are provisioned or when re-optimizing the network. OPMs and an active control plane are also helpful in anticipating, identifying and remedying the QoT problems that could occur later.

In this paper, we start by presenting a model for equipment ageing and proceed to describe an economic cost model appropriate for evaluating the benefits of postponing the purchase of equipment. We then present an algorithm that incrementally plans the network and provisions lightpaths based on actual (measured) physical layer conditions, with just enough margins, that is with actual system (ageing and interference) and reduced design margins. Using the actual margins, the algorithm optimizes the decisions on the placement and the transmission parameters of the configurable transponders (also referred to as Bandwidth Variable Transponders – BVT) and regenerators including their launch powers. The proposed algorithm is suitable for incrementally planning a network over multiple periods, it is quite generic, and can be used with configurable and non-configurable (fixed) transponders as well.

Using the proposed algorithm, we evaluate the gains of provisioning lightpaths with actual margins in an incremental multi-period planning scenario, for an Elastic and a Mixed Line Rate (MLR) network. For comparison purposes, we consider the related scenarios that use worst-case margins. Our results indicate that provisioning with actual margins and just in time can yield significant cost savings that accumulate to 36% at the end of the examined periods for an Elastic and 51% for a MLR network. These savings increase to 41% and 58%, respectively, if we consider 2.5% interest per year on saved investment.

The rest of the paper is organized as follows. Section II reports on related work. Section III discusses QoT and margins, and describes the ageing model used in our techno-economic study. Section IV presents our cost model. Section V presents the heuristic algorithm for network planning with actual margins. Finally, Section VI presents the performance comparison results, followed by our conclusions in Section VII.

II. Related Work

Provisioning lightpaths based on the actual network conditions and the actual capabilities of equipment, instead of making worst-case assumptions and using EOL margins, has attracted recent attention from the research and industrial community. Different approaches have been proposed both for WDM [10]–[12] and Elastic optical networks [7], [13]–[16].

Initially, researchers focused on WDM networks with the authors in [10] presenting a hierarchical routing and wavelength assignment (RWA) algorithm that takes into account estimates of the current optical signal-to-noise ratio (OSNR) and polarization mode dispersion (PMD) effects. In [11], different wavelength assignment techniques, such as crosstalk aware (CTA)-random pick, CTA-first-fit, CTA-most-used, CTA-least-used, that co-operate with a RWA algorithm were proposed. The proposed schemes select the wavelength causing the least crosstalk on the new and existing connections. The authors in [12] proposed optimal RWA algorithms based on Integer linear programming (ILP) RWA formulations that take into account the PLIs, including both path-dependent (ASE, XCI, etc.) and interference-dependent (XCI and XT) ones, through additional ILP constraints.

As Elastic optical networks gained ground, the effort was transferred to developing routing and spectrum allocation (RSA) algorithms that use reduced margins. Specifically, the authors in [13] aimed at increasing network throughput by accounting for nonlinear impairments (NLIs) when optimizing individual transmission parameters and spectral channel allocation. Two flexibility parameters of the BVT transponders were examined, namely, the launch power and the FEC code, and their impact on the SNR was investigated. Reduced margins, obtained by avoiding the consideration of future losses, were examined in [14], where the advantages arising in terms of spectrum usage and capacity on the first day of network operation were investigated. The authors of [15] developed an algorithm that minimizes the launch power, which is maintained end-to-end, thus indirectly minimizing interference PLIs. In a similar manner, [16] focused on RSA and end-to-end power optimization, to reduce the effect of NLIs. End-to-end power optimization for each channel and the related margins are also studied in [17], while (local) per span power optimization assuming not full compensation of the attenuation is reported in [18]. To reduce interference in Elastic networks, another approach is to use spectrum guard bands, trading off spectrum utilization for reach when needed. Using a wider set of transmission options that account for spectrum guard band, the RSA algorithm in [19] harvests spectrum/interference trade-offs to plan the network with reduced cost. The authors in [7] quantify the related cost savings when using Elastic transponders to fit dynamically the ageing degradation as opposed to planning with EOL ageing margins.

A key idea exhibited in the aforementioned papers is that of provisioning lightpaths close to the actual/current conditions, which include actual ageing of equipment but also actual (based on currently established lightpaths) interference. This corresponds to using actual, instead of EOL, system margins. For this purpose, we need to use a Q-tool, a QoT estimation model, and feed it with current ageing and network utilization parameters.

QoT estimation models range from analytical to simulations. Recently the Gaussian Noise (GN) model [21] has been introduced and shown to be quite accurate, while its approximated closed form analytical version [22] combines good accuracy and low computational complexity. Since models cannot capture all the physical details, and also it is hard to know precisely all network parameters, the design margin is used additionally to capture such inaccuracies.

The capability to continuously monitor the network and the QoT of established connections is the key to reducing both the system and the design margins. For example, we can use a feedback-based QoT estimation approach, like the one proposed in [9], which correlates the monitored QoT values of established lightpaths to estimate the QoT of new lightpaths. As the network evolves with time and more lightpaths are established, more information become available (since each new lightpath is also monitored), the physical state is better understood and QoT estimates become more accurate with actual system and lower design margins. Alternatively, monitoring can be used to reduce the uncertainty of the parameters used as input in the Q-tool model and thus reduce the design margin [20].

The contribution of our paper is fourfold. First, we introduce a detailed ageing model to model the degradation due to ageing of several network components. Second, we introduce an economic cost model to evaluate the gains that can be realized for the network operators by postponing investments. Third, we propose an RSA heuristic algorithm that considers the actual PLIs, thus taking into account both actual ageing and interference. The algorithm optimizes the decisions regarding the placement and the transmission parameters of transponders and regenerators, including their launch powers. Fourth, the advantages of this approach in optimizing the required network resources are evaluated and compared to traditional planning with high margins using realistic network, traffic and physical layer assumptions.

III. Quality of Transmission and Ageing Model

In the following, we discuss issues related to PLIs, QoT and the margins used when provisioning lightpaths. We then present a network equipment ageing model that will be used to evaluate the benefits of planning with reduced margins.

A. QoT and Margins

In optical transport networks, the optical signals can transparently pass intermediate nodes (without undergoing Optical-Electrical-Optical conversion) and traverse long links. The accumulated PLIs degrade the signal, possibly rendering the QoT unacceptable and necessitating the use of regenerators at intermediate hops. From the algorithmic perspective, PLIs can be classified into those caused by inter-channel interference from co-propagating lightpaths (XT, XCI and MCI), and those that do not depend on other lightpaths (ASE, SCI, dispersion effects). Apart from inter-channel interference, which increases with the establishment of new connections, equipment ageing also deteriorates the QoT of the lightpaths as time passes.

A typical approach used to ensure uninterrupted transmission is to provision lightpaths with *EOL system margins* [3], [4]. In practice, the lightpaths are provisioned by calculating their QoT under worst-case interference and ageing. For interference, the typical worst-case assumption made is that all (or a large percentage of) channels are lighted. For ageing, the parameters used for fiber and equipment (transponders and amplifiers) are typically their EOL values provided by some ageing model (such an ageing model will be presented in this section).

In addition to the above discussed EOL system margins, there are two other types of margins [3], [4]: (i) the *unallocated margin*, pertaining to the mismatch of the capacity-distance of the demands and the capabilities of the transponders, and (ii) the *design margin*, pertaining to the inaccuracies of the Q-tool, the simplification of the model as well as some uncertainties in the field and equipment parameters.

Reducing the different types of margins increases network efficiency and leads to significant economic benefits, to be discussed in the following. With the evolution of flex-grid technology and configurable transponders (will be referred to as BVTs interchangeably), the unallocated margins are reduced thanks to the larger number of available transmission options. A key factor in reducing the system and design margins is to obtain a better knowledge of the physical layer, which can come through Optical Performance Monitors (OPM). Note that coherent receivers deployed today in optical networks can be extended to operate as OPMs [7]. OPMs can obtain QoT estimates that include the actual ageing and interference state of the network, which, if used in a multi-period planning scenario can reduce the system margins. Moreover, OPMs give a better understanding of the network, and if enough information is available, the Q-tool inaccuracies and thus the design margin can also be reduced [9], [20].

To provision lightpaths with *reduced* (or *actual* or *just-enough*) margins, an appropriate RWA or RSA algorithm, combined with an appropriate Q-tool, has to be used. Although the use of BVTs has a positive effect on the reduction of the unallocated margins, it increases the complexity (the problem is already NP-hard; increased complexity in this case means that its description requires substantially more variables). Moreover, due to inter-channel interference, the transmission parameters of one lightpath affect the QoT of others. Accounting for the inter-channel interference is already difficult in networks with fixed transponders [12], and becomes more complicated with BVTs. The reason is that when BVTs are used lightpaths can occupy different amounts of spectrum, making it more complicated to account for the actual inter-channel interference than in a fixed grid scenario, where all lightpaths occupy 50 GHz. Providing a heuristic algorithm that does not make worst-case assumptions is one of the major contributions of this paper.

Note that operating the network with reduced margins requires OPMs and an active control plane, to anticipate, identify and remedy QoT problems that could occur as time progresses. The design margin can play the role of avoiding operating the network right at the limit, and having connection susceptible to minor network changes.

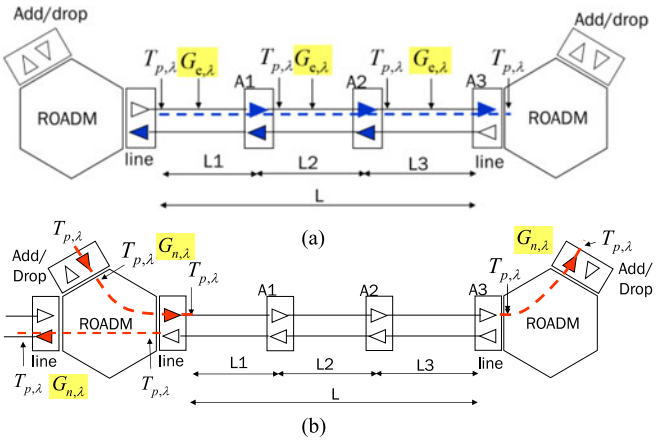

Fig. 1. OSNR model for (a) a multi span link and (b) an ROADM for add, drop and pass-through signals.

TABLE I
SYSTEM AND DESIGN MARGINS BOL AND EOL VALUES

Margin			BOL	EOL
System margins	Ageing	Fiber attenuation parameter α_{loss} (dB/km)	0.22	0.23
		Connector loss c_{loss} (dB)	0.20	0.30
		Splice loss s_{loss} (dB)	0.30	0.50
		Number of slices s_e (km^{-1})	0	0.027
		Number of connectors per span	2	2
		EDFA noise figure N_e (dB)	4.50	5.50
		OXC loss A_n (dB)	20.00	23.00
		Transponder margin M_T (dB)	1.00	1.50
	Interference		Empty	Full
Design margin M_d (dB)			2.00	1.00

B. Ageing Model

A key factor affecting a lightpaths' QoT is the degradation caused by equipment ageing. The main network components whose performance deteriorates with time are the transponders, the fibers, the optical switches and the amplifiers. As discussed above, the effect of ageing, along with interference are typically accounted through the system margins. The system margins usually account also for the degradations due to splices or extra connectors to fix fiber cuts or other types of failures. To give a reference value, [24] reports the allocation of a 3dB margin to account for EOL ageing effects.

In the following, we present a model that will be used in our studies to describe the ageing effects. This model was integrated into the GN model [21] that was assumed to describe the physical layer and was used by our RSA algorithm (presented in Section V) for estimating the QoT of the established and the new lightpaths with actual system margins. Instead of this model, OPMs combined with accurate QoT estimation methods [9] could be used in a real network, but this requires testbed/field experiments, which are outside the scope of this study.

We assume a dispersion uncompensated optical network, whose links consist of spans of single mode fiber (SMF) followed by an erbium doped fiber amplifier (EDFA) that fully compensates the span losses. Fig. 1(a) show an example of the multi-span link model. The network nodes consist of optical cross connect (OXC) switches, which are implemented as a reconfigurable optical add drop multiplexer (ROADM) based on wavelength selective switches (WSS). Many variants of ROADM architecture have been proposed and most of them are commercially available, for either fixed-grid (suitable for MLR transponders) or flex-grid (enabling Elastic networks and the use of BVTs). It is out of scope of this article to provide a detailed model for a specific ROADM implementation.

To describe our ageing model, we initially focus on a span e. Ageing affects the fiber attenuation parameter $a_{loss}(\tau)$, which is thus modeled as a function of time τ. This can be a linear or non-linear (e.g., smooth at the beginning and steep at the end) function. The span loss depends also on the traversed number of connectors and splices. Optical fiber connectors are used where connect/disconnect capability is required, while the number of splices depends on the history (fiber type, mode of deployment, suffered failures, etc). Both connector's loss $c_{loss}(\tau)$ and splice loss $s_{loss}(\tau)$ are modelled as functions of time. Also, for a specific span e we can model the number of connections $c_e(\tau)$ and splices $s_e(\tau)$ as a function of time. These can be counting random processes following specific distributions and may also depend on the span length l_e. Then the total span loss A_e is given by:

$$A_e(\tau) = l_e \cdot a_{loss}(\tau) + c_e(\tau) \cdot c_{loss}(\tau) + s_e(\tau) \cdot s_{loss}(\tau). \tag{1}$$

This loss is compensated by an EDFA at the end of the span, so that the transmission power is maintained. Assuming a lightpath over path p and using wavelength λ, with power $T_{p,\lambda}$ at the beginning of each span, the power spectral density (PSD) of the dual-polarization ASE noise is given by [22, (8)] as:

$$G_{ASE,e,\lambda}(\tau) = N_e(\tau) \cdot (A_e(\tau) - 1) \cdot h \cdot f, \tag{2}$$

where $A_e(\tau)$ is the span loss ((1)), $N_e(\tau)$ is the noise figure of the EDFA at the end of span e (also time dependent), h is Planck's constant, and $f = c/\lambda$ is the lightpaths' frequency and c is the speed of light.

Following a similar approach, we model the ageing effect of a ROADM switch. Fig. 1(b) shows the contributions of the ROADM to the noise added by the node amplifiers to the different types of traffic: add, drop and pass-through. Although the different types of traffic pass a different number of amplifiers and WSSes, to simplify our model we assume that all traffic types accumulate equal loss $A_n(\tau)$. This value is assumed to increase with time τ (filters deteriorate and node amplifiers worsen their noise figure). In Table I we show the BOL and EOL node loss for all traffic types; the power spectral density $G_{ASE,n,\lambda}$ is calculated from (2) but with the related $A_n(\tau)$ value. Therefore the total power spectral density $G_{ASE,p,\lambda}$ of the ASE noise accumulated on lightpath (p, λ) is

$$G_{ASE,p,\lambda}(\tau) = \sum_{e \in p} G_{e,\lambda}(\tau) + \sum_{n \in p} G_{n,\lambda}(\tau) \tag{3}$$

Taking the GN model as reference, we can calculate the power spectral density of the NLIs (both self and cross-channel) for each span, for the actual wavelength utilization of the span using [22, (128) and (129)]. Then assuming incoherent noise accumulation, [22, eq. (127)], we accumulate the NLI noise power over a link, and over the whole path, for the actual utilization of the links/network. We will denote by $G_{NLI,p,\lambda}(\tau)$ the accumulated NLI power spectral density of lightpath (p, λ), and assume that it is a function of time, since the network load also changes (generally increases) with time.

The OSNR of lightpath (p, λ) under the assumption of not suffering from intersymbol interference (ISI) and the occurrence of match filtering [22], and that losses are fully compensated and thus the signal power at the receiver equals the launch power $T_{p,\lambda}$ is then given by

$$OSNR_{p,\lambda}(\tau) = \frac{T_{p,\lambda}}{G_{p,\lambda}(\tau) \cdot B + G_{NLI,p,\lambda}(\tau) \cdot B}, \quad (4)$$

where B is the equivalent noise bandwidth over which OSNR is evaluated.

Note that the algorithm that will be presented in Section V can optimize the launch power $T_{p,\lambda}$ of each lightpath. From the network perspective, the ingress ROADM is responsible for bringing the launch power to the decided value. We assume full compensation of the attenuation of each span by the following EDFA. Therefore, the power at the start of each span is maintained over the whole path. Intermediate ROADMs act as equalizers and correct the non-flat amplification of EDFAs. End-to-end power optimization suits the actual margin approach followed in this paper, and is also studied in [15]–[17]. The proposed optimization approach differs from the LOGON approach [18] that performs (local) power optimization per span assuming worst case interference. The calculations for $G_{NLI,p,\lambda}(\tau)$ and $OSNR_{p,\lambda}(\tau)$, described above take into account the decided lightpaths launch powers and thus the physical model described above is used for cases with fixed or optimized launch power.

We also model the ageing of the transponder with a margin $M_T(\tau)$ on its sensitivity, which is a function of time. Finally, we also take into account a specific design margin. In particular, we assume for all lightpaths a design margin $M_d(\tau)$ to account for QoT model inaccuracies and to also avoid operating right at the limit (ping pong effects). All ageing parameters are assumed to increase as time advances, while the design margin is assumed constant or decreasing with time. The assumption of a decreasing design margin is based on [3], [9], [20] and the fact that as time advances we can obtain a more accurate knowledge of the network and thus to estimate QoT with better accuracy.

To decide whether a lightpath (p, λ) is acceptable or not, we calculate its bit error rate

$$BER_{p,\lambda}(\tau) = \Psi(OSNR_{p,\lambda}(\tau) - M_T(\tau) - M_d(\tau)) \quad (5)$$

and compare it against the FECs limit BER_{limit}, where Ψ is a suitable function that takes into account the baud-rate and the modulation format of the specific lightpath, as in [27]. The lightpath is established if and only if it has acceptable QoT:

$$BER_{p,\lambda}(\tau) \leq BER_{\text{limit}} \quad (6)$$

To better understand the above model, it is useful to give some reference values. Table I provides values for the fiber attenuation parameter $a_{loss}(\tau)$, the connector loss $c_{loss}(\tau)$, the splice loss $s_{loss}(\tau)$, the EDFA noise figure $N_e(\tau)$, the attenuation of the node $A_n(\tau)$, the transponder margin $M_T(\tau)$ and the design margin $M_d(\tau)$ for τ = Begin-Of-life (BOL) and τ = End-of-life (EOL), found in the literature [14], [24], [26]. A typical value for the duration between BOL and EOL is taken to be 10 years. To find the values at intermediate time instants from the extreme values for BOL and EOL, we need to know the exact function of time, with the linear function (note, linear in dB) being a natural candidate choice, also used in our studies. The (mean) number $s_e(\tau)$ of splices per span was assumed in our simulations to increase linearly with span length and time, at a rate of 0.002728 splices/(year·km) [25]. The number c_e of connectors was taken to be constant and equal to 2 per span, placed at the two ends of the link. Note that this number depends on the connect/disconnect capabilities required by the network operator, and 2 connectors is considered the default.

Note that (3) considers only the ASE noise from EDFAs (inline and in switches), as well as the additional degradations due to ageing effects of fibers, EDFAs, switches, splices and connectors. The NLI PLIs are decoupled according to the GN model and are included in the $G_{NLI}(\tau)$. In our study, the ageing model along with the transponder and design margins ((5)) are integrated in the approximate version of the GN model for non-identical channels [22] that accounts for the actual interference (nonlinear interference and linear crosstalk) of the network when calculating the QoT feasibility of the lightpaths.

IV. Cost Model

We examine the incremental multi-period network planning problem [28], where at the start of each period new equipment is installed, depending on the new traffic and on the feasibility of the previously established lightpaths. Provisioning with actual margins allows us to start with less equipment and add more at later periods, if and when needed. An advantage of this incremental approach is that it depends only on the current and previous network state. This is in contrast to the all-periods planning problem that aims at minimizing network cost over all periods once, but requires forecasting the demands for all periods. Planning the network using traffic forecasts could yield benefits additional to the ones recorded in the current paper and is left for future work.

The benefits of provisioning with actual margins and continuously re-optimizing the network are manifold. First, equipment prices fall with time, and purchasing equipment later in time is usually cheaper. Moreover, we obtain gains from the time value of money; assuming that the capital exists, interest is obtained on postponed investment; assuming that equipment is partially purchased with loaned money, which is the typical case, a lower loan will be required and we save by avoiding paying interest on loaned money. Also, importantly, as time progresses, new and better equipment becomes available, and by deploying those, we achieve a gradual network upgrade. In general,

observing the network and upgrading just in time, when actually required, is the safest way to reduce costs and offers better services.

To account for the economic savings that can be achieved we compare two different scenarios: (i) provisioning with worst case (WM) margins, (ii) provisioning with actual margins (AM), which assumes a network that monitors itself, provisions lightpaths with just enough QoT, and places new equipment only when actually needed. As discussed above, this can be done using OPMs and an active control plane combined with appropriate RWA/RSA to postpone purchases until they are actually needed.

In our study, we compare the two provisioning scenarios in an incremental multi-period network planning scenario, with traffic and ageing effects increasing with time. In provisioning with worst-case margins (WM), equipment is added at intermediate periods only to serve the new traffic itself, since increased interference and ageing cannot turn infeasible the lightpaths provisioned in previous periods. On the other hand, in provisioning with actual margins (AM), equipment is added to account also for QoT problems that may appear as the network evolves. Note that transponders already have the ability of monitoring the performance of the related lightpaths; They use powerful ASICs to implement digital signal processing (DSP) operations to mitigate dispersion effects and demodulate the coherent signal. To enable the required OPM features, limited if any extensions to the DSP algorithms are needed, while extra software is required to transfer and analyze the OPM related information. The cost of such software is almost negligible; commercial management platforms report dispersion, BER and FEC related metrics. Moreover, ORCHESTRA has prototyped such a monitoring and control plane and used it in proof-of-concept experiments [30], [31].

For period τ_{i} we denote by $IC^{AM}(\tau_i)$ the incremental CAPEX cost of all equipment (transponders, regenerators, EDFA, WSS, etc.) incurred by scenario AM. This is given by

$$IC^{AM}(\tau_i) = IC^{New,AM}(\tau_i) + IC^{QoT,AM}(\tau_i), \qquad (7)$$

where $IC^{New,AM}(\tau_i)$ is the cost of new equipment required to serve the increased traffic demand and $IC^{QoT,AM}(\tau_i)$ is the cost of the equipment (e.g., regenerators) necessary to restore the QoT of lightpaths provisioned in previous periods with reduced margins that at τ_{i} perform with insufficient QoT.

Clearly, we have $IC^{New,AM}(\tau_i) \leq IC^{WM}(\tau_i)$, since for the same new traffic, higher margins are used in WM scenario. The incremental cost of the devices that will be required in the future under scenario AM will allow money savings with respect to scenario WM, because these devices (preventively installed under scenario WM) will either (a) never be used under scenario AM, or (b) their cost will have decreased by the time they are deployed. Finally, it is important to account for the time value of money.

TABLE II
PROJECTIONS A AND B FOR THE NUMBER OF 100 GBPS FIXED-TRANSPONDER UNITS AND RESULTING PRICES ASSUMING LEARNING RATES $R = 0.85$ FOR PROJECTION A AND $R = 0.75$ FOR PROJECTION B

	Year	τ_0	τ_{0+2}	τ_{0+4}	τ_{0+6}	τ_{0+8}	τ_{0+10}
Projection A	Units (K)	4	5	7	10	7	
	Price (C.U.)	1	0.72	0.60	0.52	0.47	0.44
Projection B	Units (K)	5	6	10	8	7	
	Price (C.U.)	1	0.51	0.38	0.29	0.25	0.23

The accumulated total cost at the end of period τ_{n} for the two (WM and AM) scenarios, are given by:

$$TC^{WM}(\tau_n) = \sum_{i=0}^{n} IC^{WM}(\tau_i) \qquad (8)$$

$$TC^{AM}(\tau_n) = C^{mon} + \sum_{i=0}^{n} IC^{AM}(\tau_i) - I \cdot \sum_{i=1}^{n} \left[IC^{WC}(\tau_{i-1}) - IC^{AM}(\tau_{i-1})\right] \qquad (9)$$

where I is the interest rate, and C^{mon} is the cost of OPMs.

Regarding the price evolution of network equipment, we adopted Wright's Cumulative Average Model based on learning curves [29]. In the following we denote with Q a type of network equipment, which can be a transponder, regenerator, EDFA, WSS, etc. According to the learning curve model, the price of equipment Q at the start of period τ_i is approximated by

$$c^Q(\tau_i) = c^Q(\tau_0) \cdot (u^Q(\tau_i))^{\log_2 R} \qquad (10)$$

where $c^Q(\tau_0)$ is the initial price of the equipment Q, $u^Q(\tau_i)$ is the cumulative number of equipment units produced until period τ_i, and R is the learning rate expressed as decimal. The basic concept of this model is that the cost of performing a task (e.g., producing a transponder) decreases at a constant rate as the cumulative output of the task doubles. The learning rate intuitively represents how fast we learn to perform the task, that is, how fast the related cost decreases.

Based on this model, the price evolution of equipment depends on the number of units that are produced. For example, Table II shows two projections of the number of 100 Gbps fixed transponder units, called projection A and B. For projection A we fitted the number of transponders produced for year 2014 (considered to be τ_0) the predicted number of transponders for 2019 according to [32]. Then assuming a learning rate of $R = 0.85$ we forecasted the prices of the 100 Gbps transponders (second row of Table II). The prices are given in cost units (C.U.), where 1 C.U. is defined as the cost of the 100 Gbps transponder at τ_0. Under projection B, we forecasted the prices

assuming a more optimistic scenario: a higher learning rate, set to $R = 0.75$, and a heavy early production. The main difference is the steeper price drop in the first periods for Projection B. Taking a similar approach, we can calculate the forecasted prices of other equipment.

The accumulated total cost, as in (7)–(9), is the sum of all the costs of the used equipment Q (transponders, regenerators, EDFAs, WSSs, etc). Note that collecting information and projecting the production for different types of equipment is quite hard. So, in our studies we assumed that all types of transponders (even BVTs) and other equipment follow a similar unit production pattern as projections A and B for the 100 Gbps transponder presented in the above table. Since, as shown in our performance results, the cost of transponders and regenerators is the most dominant parameter, the use of different projections for the other equipment would have almost no effect on the results.

As the network evolves with time, new equipment needs to be installed due to traffic increase (under both scenarios WM and AM) or due to QoT problems (under only scenario AM), as captured in the above cost model [(8) and (9)]. Already installed equipment is assumed fully re-usable and not permanently installed in a location, that is, it can be relocated. For example, transponders and regenerators can be transferred to other nodes than those they were used in previous periods, if that is required. The cost model can be extended in a straightforward way to penalize such transfers or completely forbid them to capture operator's intention to refrain from transponder relocations once they are placed in the network. In the current study, we decided to neglect it to avoid complicating further the reader. What is more, in the studied traffic scenario a demand introduced at a given period remained for the remaining periods while new demands were later added. The proposed algorithm was observed to avoid most relocations in such a traffic scenario.

V. Incremental Multi-Period Planning With Reduced Margins

We now present a routing and spectrum allocation (RSA) algorithm that can be used to provision lightpaths with actual (just-enough) margins in an incremental multi-period network planning scenario (scenario AM in Section IV). The proposed algorithm is quite generic and although is described for flex-grid and BVTs it can be used for fixed- grid networks with fixed transponders. The algorithm has a pre-processing phase, in which the actual ageing effects and the worst inter-channel interference are considered, so as to decide on the candidate placement of regenerators. Then the RSA algorithm chooses transponders, transmission configurations, regeneration points, and assigns paths and spectrum. When the RSA allocates the spectrum it (re-) evaluates the QoT, taking into account the actual interference.

A. Problem Description

The optical network is described by graph $G = (V,\ E)$, where V denotes the set of optical nodes and E the set of optical links. The spectrum is divided into spectrum slots of z GHz, where one spectrum slot corresponds to the finer switching granularity of the flexible network elements (flex-grid switches and BVTs), and the network supports a total of F slots. We assume a traffic scenario where at the start of period τ_i we have a list of client demands. A demand is represented by the number $\Lambda_{s,d,r}(\tau_i)$ of connections between source-destination pair (s, d) with client rate r at the start of period τ_i.

Traffic is served by BVTs that control some or all of the following parameters: (a) modulation format, (b) baud rate, (c) transmission power and (d) FEC. A possible transmission configuration is described by a tuple $t = \{MF_t,\ BR_t,\ TP_t,\ OV_t\}$. The modulation format MF_t (bits/symbol) describes the number of bits encoded in a symbol, and the baud rate BR_t (symbols/sec) describes the number of transmitted symbols per sec. Thus, the total transmission rate of a given tuple t equals $MF_t\, BR_t$. The transmission power TP_t (mW), when the transmission configuration is selected for a lightpath (p, λ) equals to $T_{p,\lambda}$ as discussed in Section III. Finally, the FEC overhead OV_t is expressed as a decimal. Based on that the useful/net datarate DR_t is

$$DR_t = MF_t \cdot BR_t \cdot (1 - OV_t) \tag{11}$$

We assume Nyquist WDM transmission, and thus a tuple requires $\lceil BR_t \cdot (1 + y)/z \rceil$ spectrum slots, assuming a bandwidth overhead factor y to account for non-ideal pulse shaping and filters and spectrum slots of width equal to z.

The set T includes all possible transmission tuples t for a transponder, and the RSA algorithm has to choose one of these options to serve a demand. The above description remains valid even for fixed transponders; a fixed transponder is characterized by a single tuple. Different fixed transponders with different capabilities can also be modeled for a so called mixed line rate (MLR) scenario.

The proposed RSA algorithm at the start of a given period τ_i takes into account the previously installed (up to and including τ_{i-1}) equipment, and provisions one or more transparent or translucent lightpaths to serve each demand. To do so, it must allocate one or more transponders (according to the demand), choose their transmission configurations, place regenerators if needed, choose the path and allocate spectrum, taking into account the physical layer. To speed up the algorithm's execution time it is vital to reduce the search space and so our proposed heuristic provisions lightpaths by choosing from pre-calculated (path, transmission tuple, regeneration points) triples for each demand (see pre-processing phase in the next subsection).

The objective is to serve the traffic and minimize the accumulated cost, as described by the cost model of Section IV and (9). As a secondary objective, we can also minimize the maximum utilized spectrum to avoid running out of spectrum, which would e.g., require the addition of new fibers and the related equipment (WSSs, EDFAs, etc). Note that in the incremental multi-period planning problem that we examine, we upgrade the network at each period, assuming that no estimates are available for the future traffic. So, the overall cost, given by (9), can be calculated only for the period that we execute the algorithm. Future work will include the development of an RSA algorithm for all-periods planning to achieve the global optimum [28].

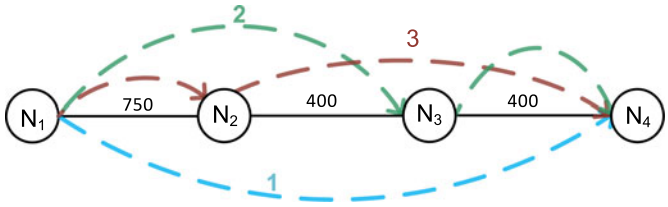

Fig. 2. Candidate end-to-end connections without or with the use of regenerators based on the upper and lower reach bounds.

B. Pre-Processing Phase

The pre-processing phase calculates candidate (path, transmission tuple, regeneration points) triples that can be used to serve a demand. For each source-destination pair (s, d) we pre-calculate k paths using a variation of the k-shortest path algorithm. We let P_{sd} be the set of candidate paths for (s, d). Then for each demand $\Lambda_{s,d,r}(\tau_i)$ which require end-to-end connections of client rate r between s and d for period τ_i, we have a number of available candidate tuples t, those with effective datarate DR_t, according to (11), which is equal to r. Note that an end-to-end connection corresponds either to a transparent lightpath or a translucent (i.e., requiring regenerators) connection. If regenerators are placed, two consecutive regeneration points define a sub-path between them, which is a transparent lightpath. Since the transmission reach depends on the current network state (including ageing and interference), but we have not yet allocated spectrum and not decided on the transmission power of the lightpaths, in the pre-processing phase we calculate the possible nodes where regenerators can be placed, taking only actual ageing into account. To do so, we pre-calculate for each transmission tuple the best and the worst transmission reaches. For a transmission tuple t, the best reach at time τ_i, denoted by $\overline{D_t}(\tau_i)$, is calculated for current (at τ_i) ageing parameters considering all PLIs that do not depend on inter-channel interference. The worst reach, denoted by $\underline{D_t}(\tau_i)$, is calculated for current (at τ_i) ageing parameters and worst-case (EOL) inter-channel interference, that is for fully loaded links.

Then, given a demand, for each (path-transmission tuple) pair (p, t), we can decide if the demand can be served in a transparent or translucent manner. In particular, assuming a path of length D_p the following cases arise:

1) $\overline{D_t}(\tau_i) < D_p$; we need to deploy regenerators,
2) $\overline{D_t}(\tau_i) > D_p > \underline{D_t}(\tau_i)$; interference must be estimated to decide whether to transmit transparently or translucently;
3) $\underline{D_t}(\tau_i) > D_p$; we can transmit transparently and we do not need regenerators.

According to the above classification, if regenerators are needed or might be needed (cases (i) and (ii), respectively), we keep all possible placements of regenerators for the related upper and lower reach bounds. A candidate placement of regenerators is denoted by *m*, and thus (p, t, m) represents a candidate (path, transmission tuple, regeneration points) triple to serve the demand.

Fig. 2 shows an example of this operation. Assuming a connection from node N_1 to node N_4 over path $p = \mathrm{N}_1{-}\mathrm{N}_2{-}\mathrm{N}_3{-}\mathrm{N}_4$ with length $D_p = 1700$ km. Assuming a transmission tuple t with DP-16QAM, 32 Gbaud, 0 dBm, 22% overhead, at time τ_0 the best (BOL) transmission reach is $\overline{D_t}(\tau_0) = 1900$ km, while EOL margins yield reach $\underline{D_t}(\tau_0) = 900$. Since interference effects depend on network utilization and are unknown at this point, taking into account the aforementioned best and worst case distances we define the candidate regeneration points m. The end-to-end communication can be established either transparently, as depicted in connection 1 ($m = \{\}$), or translucently, as shown in connections 2 ($m = \{\mathrm{N}_3\}$ and 3 ($m = \{\mathrm{N}_3\}$). So for the path and transmission tuple at hand we create 3 candidate (p, t, m) triples.

Note that in the case of long links where QoT is not acceptable over that single link we assumed that we could place regenerators at the end of some spans along the link where needed. In that case, we allocated the same spectrum on all the spans of the link. This does not affect the performance of the algorithm; no traffic is added at the regeneration point in the middle of a link, and so no gain can be achieved by re-allocating the spectrum at that point.

Keeping and considering all regeneration options for cases (i) and (ii) is important. For example, certain links might have several spectrum-neighbouring lightpaths with high power, while others may be used by fewer lightpaths with lower power. So deciding on the regenerators' placement without taking into consideration the network state (spectrum allocation and power) is rather sub-optimal, and is not done in this pre-processing phase but left to be performed by the RSA algorithm (described in the next sub-section).

So, in the pre-processing phase, for period τ_i for each demand $\Lambda_{s,d,r}(\tau_i)$, we calculate a set $Q_{s,d,r}(\tau_i)$ of feasible (path, transmission tuple, regeneration points) triples, each represented by (*p*,*t*,*m*), where $mm \in R_{p,t}$, taking into account the current ageing of the network. The cost $C_{p,t,m}(\tau_i)$ of a triple (p, t, m) is

$$C_{p,t,m}(\tau_i) = \Lambda_{s,d,r}(\tau_i) \cdot (c^T(\tau_i) + n_{p,t,m}(\tau_i) \cdot c^R(\tau_i)) \quad (12)$$

where $c^T(\tau_i)$ and $c^R(\tau_i))$ are the prices of the transponder and regenerator, respectively, at time τ_i, and $n_{p,t,m}(\tau_i)$ is the number of regenerators required for each end-to-end connection for the specific regeneration points m. The prices $c^T(\tau_i)$ and $c^R(\tau_i)$ vary with time, as described by the related learning curve model [(10)].

The total spectrum required by this triple is given by

$$S_{p,t,m}(\tau_i) = L_p \cdot \Lambda_{s,d,r}(\tau_i) \cdot \lceil BR_t \cdot (1 + y)/z \rceil, \quad (13)$$

where L_p is the number of links of path p and y the overhead that accounts for the pulse shaping roll-off factor and the non-ideal filters. As discussed above, the definition of a (path, transmission tuple, regeneration points) triple accounts for current network ageing, but not for interference. Depending on the network utilization and the power allocation, a connection might be QoT feasible or not. Coarse worst and best case calculations done in the pre-processing phase enable us to identify the lightpaths that are susceptible to such problem. For those the RSA algorithm, described in the next sub-section, has to consider the actual interference when allocating spectrum and select triples

that are QoT feasible while minimizing the incremental cost of the network.

C. RSA Algorithm Description

We now describe the RSA heuristic algorithm that provisions lightpaths for the next period, taking into consideration the actual interference instead of worst-case assumptions.

A link is represented by two vectors: the slot utilization vector and the power spectral density (PSD) vector. The link slot utilization vector represents with 0 a free slot and with 1 a slot occupied by a lightpath crossing the link. The path slot utilization vector is found by applying the Boolean OR operation on the slot utilization vectors of the links that comprise it and is used for avoiding spectrum overlapping when assigning slots to new lightpaths. The PSD vector of a link takes into account the selected spectrum and power for the lightpaths that cross it and is used by the Q-tool to estimate the actual interference impairments. In our algorithm, this QoT estimation is done using the GN model [21], [22], extended as described in Section III-B to account for the ageing effects, and using the PSD vectors of the links to account for actual interference. A design margin (see Section III) is used to account for any inaccuracies. In a real network, the ageing model would be replaced with monitored values, and the GN model could be replaced by any other physical layer model or the correlation technique of [9], as long as the model could use the monitored values to obtain the actual system margins and reduce the design margin.

The proposed algorithm serves the demands one-by-one in a particular order. For each demand, it considers the (path, transmission tuple, regeneration points) pre-calculated triples that can be used to serve it. For a given triple (p, t, m), for each of the $\Lambda_{s,d,r}(\tau_i)$ end-to-end connections and the related regeneration points m, the algorithm allocates spectrum to the sub-paths (transparent lightpaths). For each sub-path, it creates the path spectrum utilization vector, and searches for spectrum voids with size larger than the slots defined by the related tuple. Note that when deciding to select a transmission tuple the algorithm also selects the transmission power of the lightpath (TP_t). Thus, deciding on the (path, transmission tuple, regeneration point) triple and on the spectrum allocation we decide on the $T_{p,\lambda}$ of (4) of Section III. This along with the PSD vectors of the links are fed to the GN model. Then the algorithm uses that to determine (i) if this sub-path is feasible and (ii) if it does not make infeasible some previously established lightpath. Otherwise, the algorithm tries to use guardband (void spectrum slots) to reduce the effect of inter-channel interference. If it fails also in that case, it deploys a regenerator at the node closer to the middle of the path.

If the selected spectrum allocation choice satisfies both these requirements, it selects it and continues, otherwise it searches for a different spectrum allocation choice. During this process, the RSA also examines cases where spectrum space (guard band) is left between the lightpaths, which reduces interference effects for lightpaths that are close to their QoT limit. The above process is done for all sub-paths, and when successful, the algorithm considers that (path, transmission tuple, regeneration points) triple as network- and QoT-feasible. If not successful, it continues with the next triple.

After examining all the triples for a demand, it selects the triple and the related spectrum allocation that minimize the added cost as described by the following objective:

$$\underset{(p,t,m)\in Q_{s,d,r}}{\text{Min}} \Big(w_1 \cdot C_{p,t,m}(\tau_i) + w_2 \cdot S_{p,t,m}(\tau_i) + (1 - w_1 - w_2) \cdot TP_t \Big) \tag{14}$$

In (14), w_1 and w_2 are weights used to give the desired relative importance to the optimization parameters: cost, spectrum and transmission power. Minimizing the used spectrum apart from being a typical optimization parameter, minimizes indirectly the cost of additional equipment required for the installation of new fibers, when the spectrum is consumed. The cost of such equipment is included in the calculation of the network cost [(7)–(9)]. Since such resources are shared, they should not affect the cost and the decision for one demand [(14)], and so they are indirectly accounted for through the minimization of the spectrum. Minimizing the selected transmission power reduces the inter-channel NLIs. In this way we sacrifice the reach of some lightpaths that operate in the linear regime but have abundant reach and tradeoff that for the increase of reach of certain lightpaths that actually need it. For those we can increase their launch power and since we have low NLIs we can still operate them close to their linear/nonlinear limit and obtain the extra required reach. The objective function of the proposed algorithm is designed to harvest exactly this tradeoff.

The above objective corresponds to a specific demand, and the heuristic algorithm serves all of them one-by-one, in a specific ordering, remembering the previous decisions (updating each time the links slot utilization and PSD vectors) in order to avoid spectrum overlapping and calculate the actual interference. Note that for a new lightpath that is installed, we not only check that its QoT is sufficient but also that it does not turn infeasible the lightpaths of the previous decisions. Since the order of the demands affects the cost of the solution we could use a Simulated Annealing meta-heuristic to search among different orderings for the best performing one.

The overall cost of the network is the sum of the costs $C_{p,t,m}$ of all the selected triples for all demands, and is calculated using (9). Note that in the objective function of (14), we do not subtract the cost of the previous periods, since it is the same for all examined triples (assuming no penalty for relocating transponders and regenerators and re-routing lightpaths from the previous periods). As discussed in Section IV, equipment relocation and re-routing operations can be included in the cost model. In this case, they can be also discouraged by appropriately modifying the objective in (14) to remember the equipment placed at each node and penalize such operations.

VI. Performance Results

In this section, we quantify the benefits that can be obtained by provisioning lightpaths with actual margins as opposed to provisioning with worst case margins. To do so, we conducted

TABLE III
TRANSMISSION TUPLES OF THE 400 GBPS BVT, AND THE CORRESPONDING BEST AND WORST-CASE REACHES ASSUMING 1 DBM LAUNCH POWER AND LDPC FEC

Data Rate (Gbps)	Baud Rate (Gbaud)	Mod Format	Reach (km) BOL ageing & BOL interf. & BOL design $D_t(\tau_0)$	BOL ageing & EOL interf. & BOL design $\underline{D}_t(\tau_0)$	EOL ageing& BOL interf. & BOL design $D_t(\tau_{10})$	EOL ageing & EOL interf. & BOL design $\underline{D}_t(\tau_{10})$	EOL ageing & EOL interf. & EOL design
100	16	DP-16QAM	1900	900	1100	600	700
100	32	DP-QPSK	5900	3300	2800	2000	2500
100	64	DP-BPSK	6900	4900	3000	2500	3100
200	32	DP-16QAM	1300	700	600	400	500
200	43	8QAM	1800	1100	800	600	800
200	64	DP-QPSK	3400	2400	1500	1200	1500
400	51	DP-32QAM	400	300	200	100	200
400	64	DP-16QAM	700	500	300	200	300

TABLE IV
BEST AND WORST-CASE REACHES OF THE MLR FIXED TRANSPONDERS ASSUMING 1 DBM LAUNCH POWER AND LDPC FEC

Data Rate (Gbps)	Baud Rate (Gbaud)	Mod Format	Reach (km) BOL ageing & BOL interf. & BOL design $D_t(\tau_0)$	BOL ageing & EOL interf. & BOL design $\underline{D}_t(\tau_0)$	EOL ageing & BOL interf. & BOL design $D_t(\tau_{10})$	EOL ageing & EOL interf. & BOL design $\underline{D}_t(\tau_{10})$	EOL ageing & EOL interf. & EOL design
100	32	DP-QPSK	5900	3600	2800	2100	2600
200	43	DP-8QAM	1800	1200	800	600	800
400 (2x200)	2x32	DP-16QAM	1200	800	500	400	500

simulations using the proposed RSA algorithm, presented in Section V, assuming the ageing and cost models, described in Sections III and IV, respectively.

We considered two network settings: (i) Elastic optical networks (EON) and (ii) fixed-grid WDM. In the Elastic network setting we assumed two types of BVT transponders: (i.a) a BVT that supports baud rates up to 32 Gbaud, modulates using dual polarization (DP) up to DP-16QAM and transmits up to 200 Gbps, and (i.b) a BVT that supports baud rates up to 64 Gbaud, modulates up to DP-32QAM and transmits up to 400 Gbps. Table III presents the transmission options of the 400 Gbps BVT. For the WDM network, we assumed a mixed-line rate (MLR) case with three types of fixed transponders of 100, 200 and 400 Gbps transmission rates. Details regarding the modulation format and the baud rates are given in Table IV. Two different cases were assumed for the transmission power of the transponders: fixed, where all transponders have 1 dBm transmission power, and variable where each transponder can be tuned to have transmission power from the discrete set &3, &2, 1, 0, 1, 2, 3] dBm. Note that the developed algorithm requires as input a discrete set of candidate transmission options and can be used for any launch power value. Since the execution time of the algorithm depends on the set of transmission options, to obtain all the results in reasonable time we selected to limit our search to the specific set of integer launch power values. Note that the algorithm is polynomial, but we simulated hundreds of periods for a big network; for a single period the algorithm can examine a much wider set of launch power options in a few to a few tens of minutes. All transmission configurations use the LDPC (4161, 3431,0.825) FEC code, with 21.2% overhead with pre-FEC BER limit of 10^{-2}. The bandwidth overhead for non-ideal pulse shaping and filters was selected to be $y = 0.15$ (13). The width of the spectrum slot was taken to be $z = 12.5$ GHz and we assumed that each fiber link supports $F = 320$ slots/fiber for the Elastic network setting, while for the fixed-grid we had $z = 50$ GHz and $F = 80$ wavelengths/fiber.

Fig. 3. The network topology used in the multi period planning study.

In our simulations, we used a topology inspired by Telecom Italia's European backbone, shown in Fig. 3. We assumed that the network employs ROADMs and uncompensated SMF links. The amplification span was taken 100 km, and each span was followed by an EDFA that fully compensated the attenuation of the previous span. The gain of the EDFAs were assumed flat (we did not consider gain ripple/tilting effects). To model the physical layer, we extended the GN model and integrated the equipment ageing model, as presented in Section III. We used the margin parameters reported in Table I, which give the values for the two extreme time instants (BOL and EOL); the values for intermediate time instants were found through linear (in time and in dB) interpolation. New or existing transponders can be used to serve the demand for the different periods, consequently when new transmitters/ regenerators are deployed at intermediate periods their related ageing margin is counted from the specific period of deployment.

A multi-period incremental analysis for 10 periods was carried out, while the results are presented with a step of 2 periods. Each period can correspond to a year, but in our results, we keep for generality the term period. We assumed total traffic varying from 20 to 186.3 Tbps for the 10 simulated periods and 25% compound growth rate (CAGR) per 1 period. The contribution of each client rate to the total traffic carried in the network for the different periods is presented in Fig. 4. These client rates are matched with equal line rate transponders, as captured by the appropriate definition of the demands $\Lambda_{s,d,r}$ which are matched with equal rate tuples, as described in Section V. Note that we did not assume client side grooming (e.g., the use of muxponders). In the case of the Elastic network, since BVTs are configurable, we assumed that they could re-tune between periods serving different client connections. We also assumed

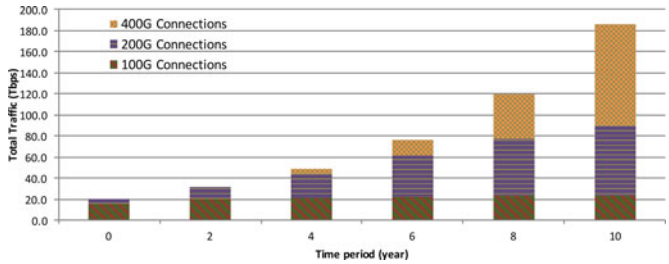

Fig. 4. Total traffic in Tb/s carried in the network expressed in number of different client rates per simulating period.

that 400 Gbps (BVT and fixed) transponders become available at period 4.

In Table III, we present the transmission capabilities of the 400 Gbps BVT used in the Elastic network setting and the related reach for the best $\overline{D_t}(\tau_0)$ (BOL ageing and BOL interference) and worst $\underline{D_t}(\tau_0)$ (BOL ageing and EOL interference) cases at τ_0 for transmission launch power equal to 1 dBm. For the worst interference scenarios, we assumed 60 lightpaths on each link, densely spaced and all transmitting at 1 dBm. Note that the contribution of XCI becomes less important as the channels frequency distance increases, while due to slot/wavelength continuity constraint the utilization of the spectrum is not continuous, thus 60 densely spaced lightpath are considered appropriate to model the worst case. Regarding the launch power although when optimizing the power certain lightpaths can exceed 1 dBm, as will be shown in the results, in all examined cases the average launch power was close to 1 dBm. Moreover, in this way we exclude examining solutions with very high interference (average higher than 1 dBm), keeping the lightpaths in the linear regime. We also present the related transmission reaches for the last period τ_{10}, $\overline{D_t}(\tau_{10})$ (EOL ageing and BOL interference) and $\underline{D_t}(\tau_{10})$ (EOL ageing and EOL interference) and assuming BOL design margin. We also present the calculated reaches for the last period τ_{10} assuming EOL ageing and interference and EOL design margin (last column). Note that, in accordance to Table I, both ageing and interference system margins increase (worsen) as time advances and we move from BOL to EOL, while the opposite happens with the design margin. The design margin reduces (improves) from BOL to EOL, assuming that as time advances we obtain a better understanding of the network parameters.

Table IV shows the same parameters for the three fixed transponders, which were assumed for the MLR WDM, network setting. Note that the EOL interference reaches ($\underline{D_t}$) are higher than the related ones for the BVT, since lightpaths are spaced in the MLR scenario in 50 GHz, instead of 12.5 GHz for the BVT, with the unused spectrum acting as guard band. Also note that the 400 Gbps fixed transponder utilizes two carriers of 50 GHz each, and each transmitting at 200 Gbps. Consequently, its reach is close to that of the related 200 Gbps BVT with the empty network exception, where the two subcarriers create inter-channel interference to each other decreasing slightly the related reach. In our simulations, we also assumed the existence of regenerators with the same capabilities with the flexible and fixed transponders that are presented in Tables III and V.

TABLE V
RELATIVE PRICES OF EQUIPMENT VALUES AT TIME τ_0

Network equipment (Q)	Unitary price (C.U.)
100 Gbps fixed transponder/ regenerator	1.00
200 Gbps fixed transponder/ regenerator	1.20
400 Gbps fixed transponder/ regenerator (introduced at period τ_4)	1.36
Flexible transponder/ regenerator 200 Gbps	1.44
Flexible transponder/ regenerator 400 Gbps (introduced at period τ_4)	1.64
EDFA	0.15
WSS (1x20)	0.30
WSS (1x9)	0.20

Note that the reaches presented in Tables III and IV are indicative. First, they assume only fiber spans and do not take into account the nodes, which would reduce the transmission reach. Secondly, they assume specific launch powers for all lightpaths (1 dBm) and that all neighbouring channels are active and densely spaced. In the simulations the QoT of each lightpath is calculated taking into account the OXC that it passes, and the chosen launch power of the other lightpaths (in Section VI-C).

The prices of the network equipment $c^Q(\tau_0)$ at τ_0 are presented in Table V, relative to the price at τ_0 of a 100 Gbps fixed transponder (taken to be 1 C.U.), apart for the 400 Gbps BVT and fixed transponders whose prices correspond to period τ_4 when they become available. Using these as starting values, we used the cost model of Section IV and the production projections of Table II, to compute the cost of the network equipment at the start of each period.

Regarding the ROADMs, we assumed a route and select architecture that provides *colorless, directionless and contentionless* operation. The number of WSS and EDFAs of a reference ROADM switch are given by:

$$WSS_{1x20} = 2 \cdot \left\lceil \frac{A_i}{20} \right\rceil, \tag{15}$$

$$WSS_{1x9} = 2 \cdot \left(N_i + \left\lceil \frac{A_i}{20} \right\rceil \right), \tag{16}$$

$$EDFAs = 4 \cdot \left(\left\lceil \frac{A_i}{20} \right\rceil + 2 \cdot N_i \right) \tag{17}$$

where N_i is the degree of node $ii \in V$, and A_i the number of the connections that are either added or dropped at node i. We assumed that we use two 1×20 WSS, two 1×9 WSS, and four EDFA for each add-drop terminal, and thus we use $\lceil A_i/20 \rceil$ such terminals at node i. We also assumed two 1×9 WSS and two EDFA for the fiber interfaces (1×9 WSSs are sufficient for the connectivity degree of the network nodes).

In the CAPEX calculations, in addition to the transponders, regenerators and ROADMs, we also considered the cost of the fibers assuming that they are rented, with relative cost 0.004 C.U./km/period) and the cost of inline amplifiers. Note that with the increase of the load, more transponders / regenerators are employed but also new add-drop terminals and fibers are added. In the results presented in the graphs we did not consider

TABLE VI
THE EXAMINED PLANNING VARIATIONS

	System margin - ageing	System margin - interference	Design margin
Worst margins	EOL	EOL	BOL
Actual design margin	EOL	EOL	Actual
Actual interference margin	EOL	Actual	BOL
Actual ageing margins	Actual	EOL	BOL
Actual margins	Actual	Actual	Actual

revaluation of the money $(I = 0)$ and we assumed zero extra cost for employing OPMs $(C^{mon} = 0)$.

We compare planning with worst and with actual margins for an Elastic and a fixed-grid MLR optical network. Recall that by the term actual margins we account for the effects of system (ageing and interference) and design margins. To quantify the contribution of each margin we compared the planning approaches variations listed in Table VI.

The examined planning variations have different transmission reaches as indicated in the different columns of Tables III and IV. Note that all these options have fixed launch power. In Section VI-C we will evaluate the benefits of power optimization. For obtaining the results of the actual margins variations, we used the heuristic algorithm that is described in Section V. The weighting coefficient of the algorithm's objective function was set to be $w_1 = 0.8$, $w_2 = 0.05$.

A. Accumulated Total Cost

We present in Fig. 5(a) and (b) the accumulated total cost [(8) and (9)] for the multi-period incremental planning of an Elastic and an MLR optical network assuming price projection A.

As expected for both network settings (Elastic and MLR), the *worst system and design margins* exhibits the worst performance, because it considers EOL ageing and interference system margins, and BOL design margin (2 dB flat). On the other hand the *actual margins* outperforms all the other considered cases, since it reduces all considers margins. The *actual ageing margins* comes second. The *actual interference margin* and the *actual design margin* cases achieve almost the same performance in the case of the Elastic network, while in the MLR network the *actual interference margin* is slightly better. In the Elastic network, the connections are more packed in spectrum and the deterioration due to actual or worst case interference is very similar. Thus, the gain of reducing the interference margin in the Elastic network is relatively low, as opposed to the MLR network in which the reduction of the interference margin plays a more important role.

From the above it becomes evident that the different margins contribute differently in the examined network settings and at different periods. When the different margins are jointly reduced, as the proposed *actual margins* solution does, the advantages are combined. For example, the 1dB difference at the EOL when comparing the *actual design* and the *worst system and design margins* is also harvested in the *actual margins* case.

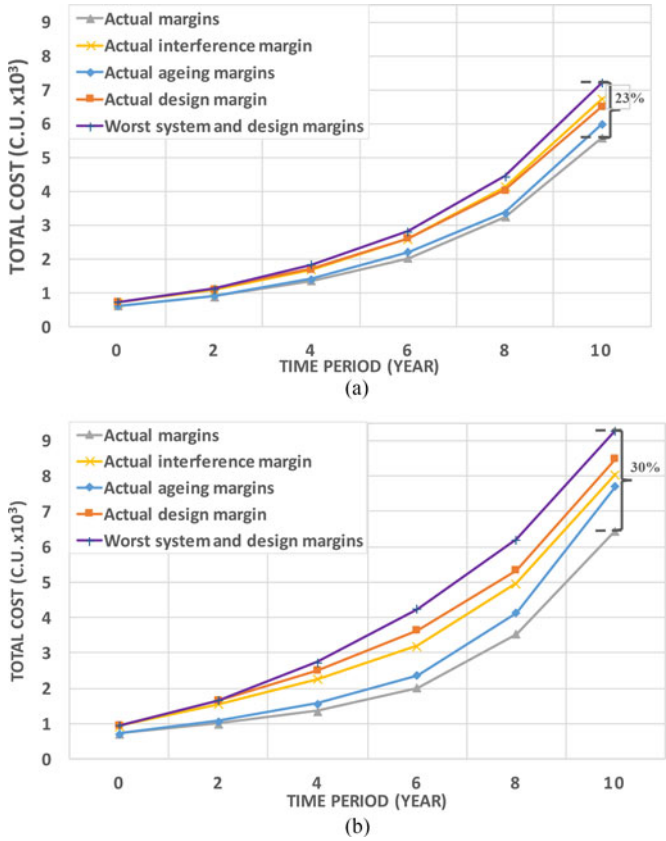

Fig. 5. The accumulated total cost (in C.U.) for the (a) Elastic, (b) MLR network for the different planning scenarios assuming price projection A for the network equipment.

To evaluate the benefits in a more quantitative way we calculate the percentage savings at the end of the examined periods, given by the following equation for $n = 10$

$$\frac{TC^{AM}(\tau_n) - TC^{WM}(\tau_n)}{TC^{AM}(\tau_n)} \cdot 100\% \tag{18}$$

For price projection A and learning rate $R = 0.85$ we obtain savings of 23% for an Elastic and 30% for an MLR optical network. The savings can be increased by investing the reserved money (or avoiding repaying loaned money with interest). So taking also into consideration an interest rate $I = 2.5\%$ per period, the savings at the end of the examined 10 periods are about 26% for the Elastic and 36% for the MLR.

Comparing the results for the Elastic and the MLR networks, we observe that initially the cost of planning the MLR with *actual margins* is close but lower than that of the Elastic. This is done by exploiting the lower prices of the fixed transponders and regenerators (100 Gbps - 1 C.U.) compared to the 200 Gbps BVT (1.44 C.U.) in the Elastic. As time passes, the cost of the MLR network increases and exceeds that of the Elastic, since there are not many transmission options and more regenerators are required to serve the increasing traffic demands. Furthermore, as the traffic increases, the Elastic exploits the tuning capabilities of the transponders to alleviate ageing and interference effects, thus saving on regenerator purchases. This makes the Elastic

more cost efficient as time progresses. In fact, at the end of the simulated periods the Elastic network planned with *actual margins* is 13% cheaper than the corresponding MLR network. Similar findings were observed for the *worst system and design margins* case and the other actual margins variations. Note that the cost savings depend on the cost of the network components and especially that of the transponders and regenarots which are the main equipment that are added over time. Thus, different price projections lead to different savings, as discussed in Section VI-B, where we examine price projection B. Although the Elastic network uses more expensive transponders and regenerators, it saves in their number, and in the end manages to achieve lower cost when compared to the MLR network setting.

In the planning scenario we examined, the demands are known in the start of each period. Since blocking is not acceptable by telecom operators, as the load increases and the spectrum is consumed at certain links extra fibers are required. In particular, an extra fiber is required from the 6th period for the *worst system and design margins*, while all the other cases require it in the 8th period. In general the spectrum utilization among the different cases is similar. The *actual margins* case achieves the best utilization with the other cases following close. Note that the placement of regenerators has a possitive advantage in the spectrum utilization, since they relax the spectrum continuity constraint.

In Fig. 6, we analyze in a per element basis the accumulated total cost for the *actual margins* and the *worst system and design margins* and for periods 2, 6 and 10. In all cases, transponders and regenerators dominate the cost. The costs of the rest of network equipment (EDFAs, WSSs and fiber rental) are significantly lower. What is more, the vast majority of that equipment is deployed at the beginning of the network and it is almost impossible to postpone its purchase. As discussed, with the increase of the network load, at certain periods and certain links, a second fiber is required, and this happens earlier for the *high margins* case than for the *actual margins* variations. This explains why the cost of deployed WSSs increases at the last periods. However, this additional cost is low compared to the cost of transponders and regenerators, while the purchases are postponed for few periods and thus the savings are very low. We also observe that the number and the cost of transponders is the same in all examined cases, since we match one transponder to each client and we do not optimize the allocation of clients onto transponders.

Thus, the key difference between *worst* and *actual margins* is the number of deployed regenerators. The number of regenerators (not shown in the graph) for the *worst margins* and the *actual ageing margins*, *actual interference margin* and *actual interference margin* cases was observed to be very close at the end of the examined periods. This stands to reason since the system margins become EOL at the last period and thus all these cases have the same reach at the EOL. Therefore, in these cases the savings come from postponing the purchase of regenerators, which are purchased when they are actually needed at lower prices. When comparing the *worst margins* with the *actual design margin* we observed that at the EOL there is a difference in the number of regenerators at the last periods. So, in this case

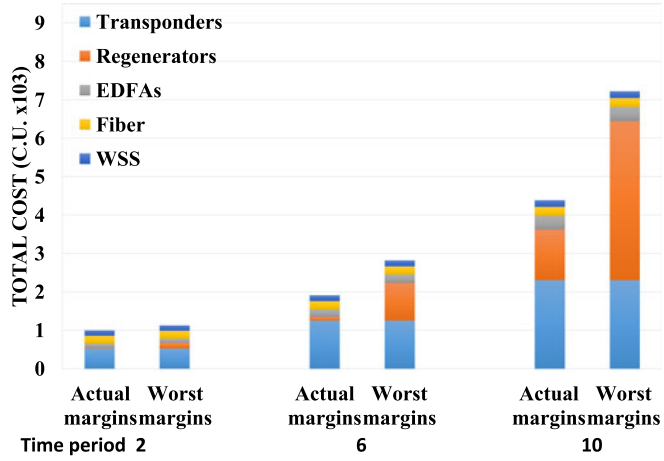

(a)

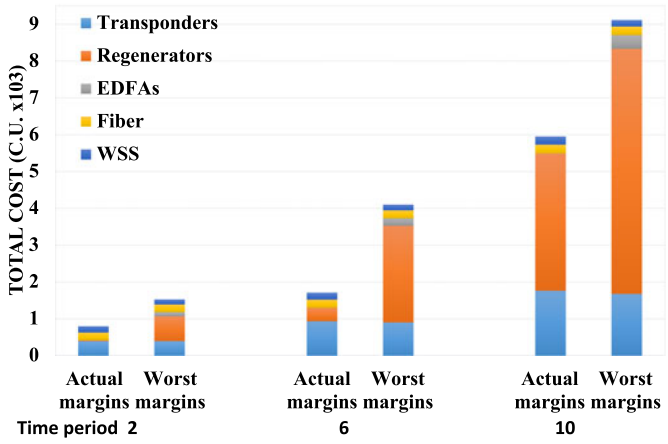

(b)

Fig. 6. The cost analysis per element (in C.U.) for the (a) Elastic, (b) MLR network for the different exploitation scenarios assuming price projection A for the network equipment.

the savings come from the fact that the *actual design margin* harvest the progressive reduction of the design margin as time advances, which ends to be 1 dB lower. In this case, we avoid purchasing some equipment, since we understand that it will not be needed to reach the EOL performance. The proposed solution, provisioning with *actual margins*, which reduces both the system and the design margins, harvests both: it postpones and avoids the purchase of equipment.

B. *Effect of Pricing Projection Model*

Fig. 7(a) and (b) show the accumulated total cost for the same network scenarios but for price projection B (Table II) with a learning rate $R = 0.75$ and a more optimistic forecast regarding the production units of the network equipment. These assumptions resulted in lower network cost per period and thus lower total cost, compared to the results reported in the previous section. This is because the regenerators are used at the latter periods when the cost is smaller affecting their relative difference between the best and worst cases. As opposed to the previous

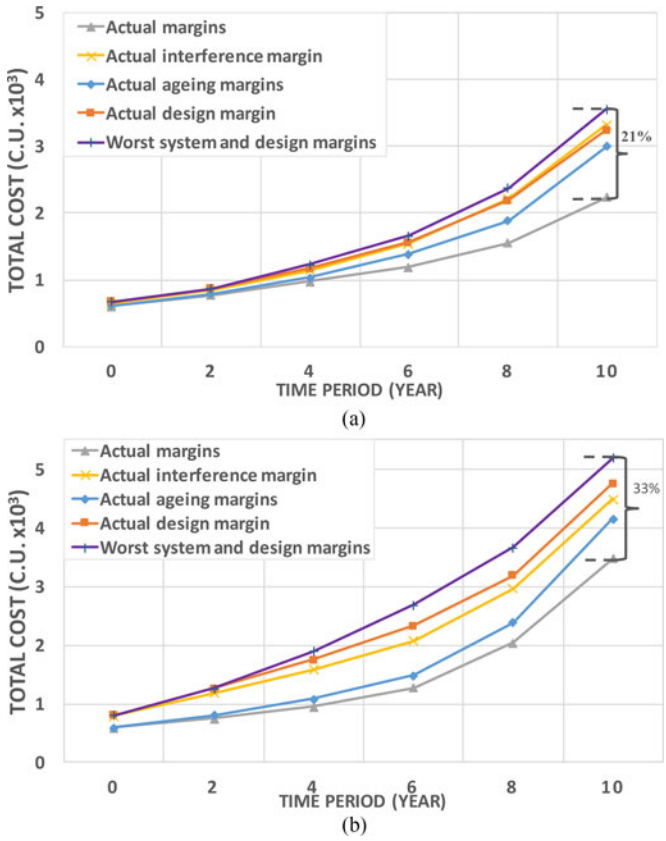

Fig. 7. The accumulated total cost (in C.U.) for the (a) Elastic, (b) MLR network for the different planning scenarios assuming price projection B for the network equipment.

case, we observe that the savings for the Elastic network reduce slightly to 21% and increase for the MLR network to 33%. The savings are 24% and 39%, for the Elastic and MLR network settings, respectively, for 2.5% interest per year.

The cost model based on learning curves that was used in this study holds with reasonable accuracy for prices that we collected of 40 Gbps transponders and 5 years. We also calculated the savings assuming a 10% equipment depreciation per year: 22% and 33% savings for the Elastic and MLR network settings were observed. Note that Fig. 6 present the number of equipment required and thus are independent of the cost model used.

Considering that Elastic constitute the most promising technology for next generation networks, a wide adaption of flexible transponders will lead to high price reductions. In such a case, provisioning with *actual margins* is highly recommended, since it leads to higher cost savings. What is more, the Elastic network seems the most adequate technology to achieve this, with the cost gains between the Elastic and MLR case to increase to 19%.

C. Launch Power Optimization

We now turn our attention to the benefits of launch power optimization. The algorithm presented in Section V for planning the network with actual margins is used but, as opposed to the previous results where the launch power was fixed to 1 dBm, the launch power of each lightpath can be chosen from the discrete set of $[-3, .. + 3]$ dBm. To account for equipment limitations, pertaining to difficulties to amplify and maintain large power differences among the channels, all the lightpaths of a specific period were allowed to tune their launch power within a window of 4 dB. For periods 0–4 the window was set to $[-3, .., +1]$ dBm, then increased by 1dB for periods 6–8, and finally, increased by 1 dB for the last period (period 10).

TABLE VII
BEST AND WORST CASE REACHES FOR THE 100 GBPS DP-QPSK TRANSMISSION OPTION FOR VARIOUS LAUNCH POWER VALUES ASSUMING NEIGHBORING CONNECTIONS OF THE SAME LAUNCH POWER

Launch power	Reach (km)				
	BOL ageing & BOL interf. & BOL design $\underline{D_t}(\tau_0)$	BOL ageing & EOL interf. & BOL design $\underline{D_t}(\tau_0)$	EOL ageing & BOL interf. & BOL design $\underline{D_t}(\tau_{10})$	EOL ageing & EOL interf. & BOL design $\underline{D_t}(\tau_{10})$	EOL ageing & EOL interf. & EOL design
-3	2800	2600	1200	1100	1400
-2	3500	3100	1500	1400	1800
-1	4300	3500	1800	1700	2100
0	5100	3600	2300	1900	2400
1	5900	3300	2800	2000	2500
2	6400	2700	3300	1800	2300
3	6200	2000	3800	1500	1900

As discussed, the launch power of a connection as well as those of the neighbouring connections affect the transmission reach of the connection at hand. The algorithm examines different (path, transmission tuple, regeneration points) triples including different launch power options of the connection at hand. It keeps only the triples that have acceptable QoT and from those it selects the one that minimizes the objective, as defined in (14), which takes into account the launch power. Therefore, the algorithm prefers lower launch power in order to indirectly reduce the NLIs and does not select the triple that optimizes the reach.

In Table VII, we present the transmission reach for the 100 Gbps DP-QPSK lightpath as a function of its launch power, assuming also equal launch powers for the neighbouring connections. We observe that the optimum launch power differs for the different margin scenarios. As expected the optimum power is lower the higher the interference is (comparing first with second columns and third with fourth columns). In addition, the optimum power increases as ageing effects increase for same interference (comparing first with third columns and second with fourth columns). Note again, that as was the case of Tables III and IV, the reaches presented in Table VII are indicative and is presented to highlight how launch power can affect the reach, since they do not take into account the nodes, and assume equal launch power for all lightpaths. Note that the algorithm examines the different launch power options for each lightpath and estimates the QoT taking into account the chosen launch powers which can be different for previously served lightpaths and also the effect of the network nodes.

The simulations showed that provisioning with *actual margins and optimized launch power* follows the trend of the actual margins case as reported in Figs. 5 and 7 with improved performance. In the end, it manages to achieve savings of 36% for the Elastic and 51% for the MLR network compared to provisioning with worst margins (results not shown in an explicit figure). Therefore, we obtain 17% and 29% higher savings with respect to the previous results with fixed launch power for the Elastic

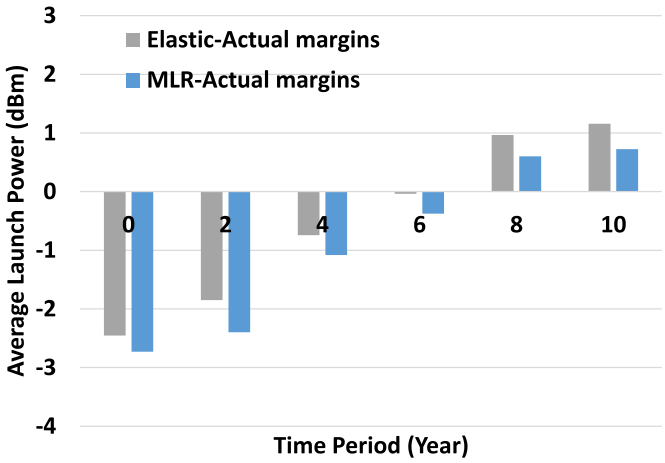

Fig. 8. The launch power used by the power optimized cases over time for the different network cases.

and MLR network settings, respectively. The savings increase to about 41% and 57%, respectively, if we also consider 2.5% interest per period.

Fig. 8 presents the average launch power per period for provisioning with *actual margins and optimized launch power* for the Elastic and MLR network settings. A similar pattern is observed for the Elastic and MLR network settings. The algorithm selects low average launch powers at the early periods and higher as time advances. This might seem counter-intuitive since as the network load increases and more connections are introduced we would expect the algorithm to reduce the launch power to reduce inter-channel interference. However, there are two factors that require higher launch power as time advances: (i) as equipment ages, extra reach is required which is obtained by increasing the launch power and moving closer to the optimum launch power values, and (ii) higher rate connections that appear as time advances use higher modulations formats and have shorter reaches and thus they need to transmit closer to their optimum launch power than lower rate connections. The effect of these two is stronger than the increase of inter-channel interference, making the algorithm to select higher launch powers as time advances. We also observe that the algorithm decides to increase the power slightly more rapidly in the Elastic network setting than the MLR. The reason for this is that in the Elastic network setting the BVTs have more transmission options and so they can achieve the required reach by harvesting some other parameter e.g., adapting the modulation format, and not only the power, as done in the MLR network setting. The graph shows an average launch power close to 1 dBm in the end of the examined periods, which was the choice for the fixed launch power cases. Our results indicate that power is an additional dimension that can be harvested by physical layer aware optimization algorithms to obtain higher benefits, as also reported in previous works [15]–[18].

VII. Conclusion

Lightpaths in optical networks are currently provisioned with worst case margins, calculated under End-of-Life (EOL) system assumptions for the ageing of equipment, interference and maintenance tasks, and also a design margin to account for estimation model inaccuracies. The impairment measuring capabilities of coherent optical transponders offer the possibility to operate the network closer to its true capabilities, improving efficiency and postponing or avoiding expenditures. To evaluate such benefits, we presented an equipment-ageing model, together with a cost model that accounts for the depreciation of equipment with time. We also proposed a routing and spectrum allocation (RSA) algorithm that provisions lightpaths taking into account the actual network conditions so as to establish them with actual (just-enough) margins. Our comparison study quantified the cost benefits of planning with actual as opposed to worst case margins as well as considering the selection of different transmission launch power in an incremental multi-period planning scenario. In particular, we observed savings of about 36% at the end of a 10 period for an Elastic optical network (EON) and 51% for a mixed line rate (MLR) network. Our results indicated that power is a dimension that physical layer aware optimization can harvest to obtain higher benefits. The savings increase to about 41% and 57%, respectively, if we also consider 2.5% interest per period (saved investment or avoiding loaning money). In a more rapid equipment depreciation scenario, the savings vary between 34%–38% for the Elastic and 50%–57% for the MLR networks, for 0% and 2.5% interest per period, respectively. Moreover, the Elastic network seems the most promising technology, with the cost gains between the Elastic and MLR case to vary between 13%–19% for the different scenarios.

References

[1] "Nokia ushers in 100G transport services era with new programmable silicon chipset and next-generation optical networking systems," Nokia, 2016. [Online]. Available: http://nokia.ly/2lwnMqQ

[2] G. P. Agrawal, *Fiber-Optic Communication Systems*, 4th ed. New York, NY, USA: Wiley, 2010.

[3] Y. Pointurier, "Design of low-margin optical networks," *J Opt. Commun. Netw.*, vol. 9, pp. A9–A17, 2017.

[4] J.-L. Auge, "Can we use flexible transponders to reduce margins?," presented at the *Optical Fiber Communication Conf.*, Anaheim, CA, USA, 2013, Paper OTu2A.1.

[5] M. Bohn *et al.*, "*Elastic optical networks: The vision of the ICT project IDEALIST*," *Future Netw. Mobile Summit*, 2013.

[6] White paper Transforming Margin into Capacity with Liquid Spectrum. [Online]. Available: http://www.ciena.com/resources/white-papers/Margin-Capacity-Liquid-Spectrum.html

[7] J. Pesic, T. Zami, P. Ramantanis, and S. Bigo, "Faster return of investment in WDM networks when elastic transponders dynamically fit ageing of link margins," presented at the *Optical Fiber Communications Conf.*, Anaheim, CA, USA, 2016, Paper M3K.2.

[8] K. Christodoulopoulos *et al.*, "ORCHESTRA—Optical performance monitoring enabling flexible networking," in *Proc. Int. Conf. Transparent Opt. Netw.*, 2015, pp. 1–4.

[9] I. Sartzetakis, K. Christodoulopoulos, C. P. Tsekrekos, D. Syvridis, and E. Varvarigos, "Quality of transmission estimation in WDM and elastic optical networks accounting for space–spectrum dependencies," *IEEE/OSA J. Opt. Commun. Netw.*, vol. 8, no. 9, pp. 676–688, Sep. 2016.

[10] H. Yurong, J. P. Heritage, and B. Mukherjee, "Connection provisioning with transmission impairment consideration in optical WDM networks with high-speed channels," *J. Lightw. Technol.*, vol. 23, no. 3, pp. 982–993, Mar. 2005.

[11] D. Tao, S. S. Subramaniam, and X. Jinghao, "Crosstalk-aware wavelength assignment in dynamic wavelength-routed optical networks," in *Proc. Int. Conf. Broadband Netw.*, 2004, pp. 140–149.

[12] K. Christodoulopoulos, K. Manousakis, and E. Varvarigos, "Offline routing and wavelength assignment in transparent WDM networks," *IEEE/ACM Trans. Netw.*, vol. 18, no. 5, pp. 1557–1570, Oct. 2010.
[13] D. Ives, P. Bayvel, and S. Savory, "Assessment of options for utilizing SNR margin to increase network data throughput," presented at the *Optical Fiber Communication Conf.*, Los Angeles, CA, USA, 2015, Paper M2I.3.
[14] A. Mitra, S. Kar, and A. Lord, "Effect of frequency granularity and link margin at 100G and beyond flexgrid optical networks," in *Proc. Nat. Conf. Commun.*, 2014, pp. 1–5.
[15] D. Rafique and D. Andrew, "Nonlinear penalties in dynamic optical networks employing autonomous transceivers," *IEEE Photon. Technol. Lett.*, vol. 23, no. 17, pp. 1213–1215, Sep. 2011.
[16] D. J. Ives, P. Bayvel, and S. J. Savory, "Adapting transmitter power and modulation format to improve optical network performance utilizing the Gaussian noise model of nonlinear impairments," *J. Lightw. Technol.*, vol. 32, no. 21, pp. 4087–4096, Nov. 2014.
[17] I. Roberts, J. M. Kahn, and D. Boertjes, "Convex channel power optimization in nonlinear WDM systems using Gaussian noise model," *J. Lightw. Technol.*, vol. 34, no. 13, pp. 3212–3222, Jul. 2017.
[18] P. Poggiolini *et al.*, "The LOGON strategy for low-complexity control plane implementation in new-generation flexible networks," presented at the *Optical Fiber Communication Conf.*, Anaheim, CA, USA, 2013, Paper OW1H.3.
[19] K. Christodoulopoulos, P. Soumplis, and E. Varvarigos, "Planning flexible optical networks under physical layer constraints," *IEEE/OSA J. Opt. Commun. Netw.*, vol. 5, no. 11, pp. 1296–1312, Nov. 2013.
[20] E. Seve, J. Pesic, C. Delezoide, and Y. Pointurier, "Learning process for reducing uncertainties on network parameters and design margins," presented at the *Optical Fiber Communications Conf.*, Los Angeles, CA, USA, 2017, Paper W4F.6.
[21] P. Poggiolini, "The GN model of non-linear propagation in uncompensated coherent optical systems," *J. Lightw. Technol.*, vol. 30, no. 24, pp. 3857–3879, Dec. 2012.
[22] P. Poggiolini, G. Bosco, A. Carena, V. Curri, Y. Jiang, and F. Forghieri, "A detailed analytical derivation of the GN model of non-linear interference in coherent optical transmission systems," Tech. Rep..
[23] A. Mitra, A. Lord, S. Kar, and P. Wright, "Effect of link margin and frequency granularity on the performance of a flexgrid optical network," in *Proc. Eur. Conf. Exhib. Opt. Commun.*, 2013, pp. 1–3.
[24] V. Alwayn, *Optical Network Design and Implementation*. Indianapolis, IN, USA: Cisco Press, 2004.
[25] M. To and P. Neusy, "Unavailability analysis of long-haul networks," *IEEE J. Sel. Areas Commun.*, vol. 12, no. 1, pp. 100–109, Jan. 1994.
[26] G. ANSI, *Optical Fiber Cabling Components Standard*, TIA/EIA 568-B.3, Mar. 1, 2000.
[27] M. Seimetz, *High-Order Modulation for Optical Fiber Transmission in Springer Series in Optical Sciences*. Berlin, Germany: Springer, 2009.
[28] C. Meusburger, D. A. Schupke, and J. Eberspacher, "Multiperiod planning for optical networks—Approaches based on cost optimization and limited budget," in *Proc. IEEE Int. Conf. Commun.*, 2008, pp. 5390–5395.
[29] W. J. Morse, "Reporting production costs that follow the learning curve phenomenon," *The Accounting Rev.*, vol. 47, no. 4, pp. 761–773, 1972.
[30] N. Sambo, F. Cugini, A. Sgambelluri, and P. Castoldi, "Monitoring plane architecture and OAM handler," *J. Lightw. Technol.*, vol. 34, no. 8, pp. 1939–1945, Apr. 2016.
[31] M. Dallaglio *et al.*, "Demonstration of a SDN-based spectrum monitoring of elastic optical networks," presented at the *Optical Fiber Communications Conf. Exhibition*, Los Angeles, CA, USA, 2017, Paper Tu3L.5.
[32] A. Schmitt, "Optical transponder market boostered as 100G arrives in force," *Infonetics*, 2012.

Polyzois Soumplis received the Graduate degree from the University of Patras, Patras, Greece, in 2010 and received the Diploma of Computer Engineer and Informatics. In 2012, he received the M.Sc. degree in computer science and engineering. He is currently working toward the Ph.D. degree. His research interests include the areas of network optimization and optical networks.

Konstantinos Christodoulopoulos received the Diploma degree in electrical and computer engineering from the National Technical University of Athens, Athens, Greece, the M.Sc. degree in advance computing from Imperial College of London, London, U.K., in 2004, and the Ph.D. degree from the Department of Computer Engineering and Informatics, University of Patras, Patras, Greece, in 2009. He is a Research Fellow in the Department of Computer Engineering and Informatics, University of Patras, Patras, Greece. He was an Adjunct Assistant Professor at the same department from 2009 to 2011, and then as a Research Fellow in the School of Computer Science and Statistics, Trinity College Dublin and as a contractor for I.B.M. Research Ireland, from 2011 to 2013. His main research interests include the areas of algorithms and protocols for optical and high-speed networks, and networks for distributed and parallel computing systems.

Marco Quagliotti received the Graduate degree in electronic engineering from Politecnico di Torino, Turin, Italy, in 1991. He was a Teacher of electronics in Italian High Schools for one year. He joined TIM (formerly CSELT and TIlab) in 1993, where he took part of the Department of Network Planning. He worked on modeling, planning, and designing of packet and circuit switched networks. His current interests include the transport network, particularly, elastic optical networks. He has been involved in several EU Projects and contributed to Working Packages dealing with architectures and design of photonic networks. He is currently participating in PANTHER, ORCHESTRA, and Metro-Haul EU financed projects. He has co-authored about 25 journal and conference publications.

Annachiara Pagano received the Graduate degree in physics in 1994, she joined TIM (formerly CSELT and TIlab) in the Department of Fiber Optics and Active Devices. She worked on high capacity transmission, solitons, wideband amplifiers, and testing of Long Haul and Ultralong Haul DWDM systems. Afterward in the Department of Transport and IP Innovation, she has been involved in several EU Projects, in scouting of new technologies, and in the validation process of equipment for domestic and Pan-European backbone optical networks. She has co-authored more than 50 journal and conference publications. Her current activities are focused on new high capacity optical access technologies for residential, business, and 5G front hauling.

Emmanouel Varvarigos received the Diploma degree in electrical and computer engineering from the National Technical University of Athens, Athens, Greece, in 1988, and the M.S. and Ph.D. degrees in electrical engineering and computer science from the Massachusetts Institute of Technology, Cambridge, MA, USA, in 1990 and 1992, respectively. He has held faculty positions at the University of California, Santa Barbara (1992–1998, as an Assistant and later an Associate Professor), and Delft University of Technology, the Netherlands (1998–2000, as an Associate Professor). In 2000, he became a Professor in the Department of Computer Engineering and Informatics, University of Patras, Patras, Greece, where he heads the Communication Networks Lab. He is also the Director of the Network Technologies Sector (NTS), Research Academic Computer Technology Institute (RA-CTI), which through its involvement in pioneering research and development projects has a major role in the development of network technologies and telematic services in Greece. He has also worked as a Researcher at Bell Communications Research and has consulted with several companies in the USA and in Europe. His research activities include the areas of protocols for high-speed networks, ad hoc networks, network services, parallel and distributed computation, and grid computing. He has served in the organizing and program committees of several international conferences, primarily in the networking area and in national committees.